

Automated Robotic Microassembly of Flexible Optical Components

B. Komati, A. Kudryavtsev, C. Clévy, G. Laurent, Brahim Tamadazte, Joël Agnus and Philippe Lutz

Abstract—This paper studies the fabrication of hybrid microcomponents through automated robotic microassembly. The robotic station used for the microassembly is presented in this paper and its use for the assembly of flexible optical microcomponents is done as a case study. Fully automated microassembly is done for better repeatability and accuracy of the tasks and to reduce the time cycle. For this reason, two complementary techniques are proposed and presented in this paper. The first technique consists of automated manipulation and insertion tasks using stereovision CAD-model based visual tracking. The second technique has been performed using hybrid force/position control and enable to perform grasping, guiding and releasing tasks in less than 1 s despite microscale specificities. These specificities are mainly manifested by the predominance of surface forces, the difficulty of integration sensors at this scale, the very small inertia of microcomponents and their high dynamics and the lack of precise models.

I. INTRODUCTION

Microassembly is used to fabricate hybrid miniaturized systems through a succession of several complex tasks realization [1]. Precise positioning and high speed are the main objectives of the microassembly. However, precise, complex and high speed microassembly tasks are difficult to achieve at the same time due to microscale specificities which are mainly manifested by the difficulty of sensor integration at this scale, the very small inertia of microsystems, their high dynamics, the predominance of surface and contact forces and the lack of precise models.

In literature, automated microassembly is proposed to overcome these specificities and to improve the quality and the speed of microassembly such as in [2] where high speed automated manipulation has been performed in less than 1s. Two main approaches have appeared for the automated microassembly. The first approach is the vision-based approach which consists of performing multi-DOF control of position [3]–[6]. The second approach consists of integrating force measurement [7] and control into microassembly [8]–[11], not only to provide local contact information of the predominant surface and contact forces at the microscale [12], but also, to control the dynamics of local interactions. These dynamic interactions are critical for applications where contact transition exists. Indeed, due to the small inertia of microcomponents, small contact force causes huge accelerations leading to their loss. In this paper, we are interested in the automation of the microassembly using both force and position control. For this reason, in this paper, we propose to combine both vision-based approach and force control

approach to perform fully automated microassembly and to overcome all of the aforementioned difficulties.

The objective of this paper is to perform automated microassembly of complex hybrid MOEMS proposed in [13]. The microassembly consists of assembling optical components into a substrate. Two flexible spring like structures (called *holder*) are used to fix the optical component mechanically in the substrate. The optical component is grasped on the holder springs which adds complexity to the task due to the flexibility of both holder and microgripper. To perform the microassembly, we propose to use two smart fingers microgripper developed with its model in [14].

To reach the objective of the paper, the following paper organization is proposed. Section II presents the experimental setup used for the microassembly. Section III presents a method of automated insertion using visual servoing. Section IV presents an hybrid force/position control approach used for automated grasping, guiding and releasing tasks. Experimental investigation of the microassembly are performed in section V. Finally, section VI concludes the paper.

II. MICROASSEMBLY SYSTEM CONFIGURATION

The objective of this section is to introduce the experimental setup, the microgripper used in the setup and the case study.

A. Experimental Setup

The experimental investigations of the microassembly tasks are performed using the robotic station shown in Fig. 1. The experimental setup is composed of large range motorized stages, fine positioning stages, rotation stages, a vacuum gripper and a Two Smart Fingers Microgripper (TSFM) which will be presented in the following. The three large range motorized stages are M-112.1DG from PI (Physik Instrumente) to perform large range X, Y and Z displacement up to 15 mm. The fine positioning stage is a P-611.3 NanoCube with 100 μm range and 1 nm in resolution with internal position sensors. Two rotation stages from SmarAct SR-3610-S with 1.1 μ° in resolution are used to adjust the alignment between the gripper and the micropart from one hand between the rails and the axis of the NanoCube from the other hand. The positioning and rotation stages are sensorized and closed loop controlled. The substrate is fixed on the fine positioning stage with a rotation stage to perform $X_n Y_n Z_n \theta_n$. The TSFM is fixed on a rotation axis which is also fixed on three axes large range motorized stages to perform $X_m Y_m Z_m \theta_m$ positioning of the system. $x_n y_n z_n$ represents a XYZ NanoCube positioning stage which will enable the

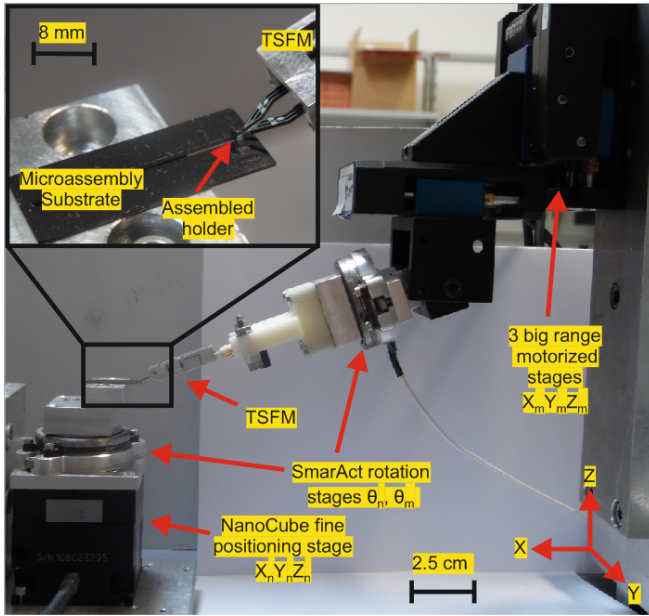


Fig. 1: Robotic microassembly station proposed for the automation of the microassembly.

positioning of the system along X and Z axes and correction of the contact force along Y axis.

B. Two Smart Fingers Microgripper

In literature, the most used solution is to integrate the force sensors inside the microgrippers because it provides gripping force measurement and it enables to locate the sensor the closer to contact. In this paper, we propose the use of two active fingers microgripper with sensorized end-effectors proposed in [14]. Indeed, the use of two-sensing-fingers microgripper provides an estimation of the lateral contact force between the manipulated micropart and the microassembly substrate in addition to the gripping forces. The microgripper used is composed of two active piezoelectric fingers [15] with integrated piezoresistive force sensors [16]. The whole gripper is called Two Smart Fingers Microgripper (TFSM). The term smart finger is used for an active material combined with integrated force sensors. The microgripper presents high bandwidth for sensing and actuation which is very important to succeed high dynamics microassembly tasks. Indeed, the dynamics of the interaction between the microgripper and the microparts are very high and consequently bandwidth of sensing and actuation have to cover these high dynamics to successfully automate the microassembly tasks.

The design, fabrication and model of the TFSM has been presented in [14]. The performances of the TFSM are summarized in Table I. A scheme of the TFSM is shown in Fig. 2 and an image is presented in Fig. 3. Fig. 2 and 3 show that each finger of the TFSM is composed of a piezoelectric actuator, rigid micropart and a piezoresistive force sensor.

Displacement	Resolution	10 nm
	Displacement range	100 μm
Force sensing	Resolution	60 nN
	Sensing range	2 mN
Bandwidth	Actuation	> 1 kHz
	Sensing	8.52 kHz

TABLE I: Performances of the TFSM fingers.

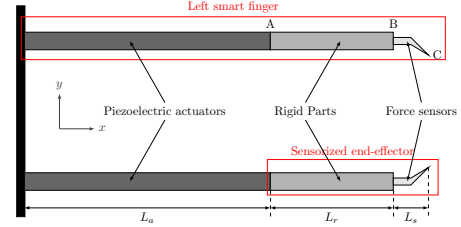


Fig. 2: Complete scheme of the two-smart-fingers microgripper (TFSM).

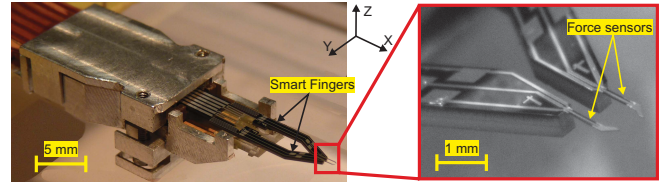


Fig. 3: Two-smart-fingers microgripper (TFSM).

C. Case study

The case study of the paper is the microassembly of hybrid MOEMS presented in [13]. These MOEMS are composed of flexible micropart called *holders* composed of an optical part and holding part with springs. The microparts dimensions are 1200 μm of height, 800 μm of width and 20 μm thickness. The main microassembly tasks are summarized in the following and in Fig. 4:

- *grasping*: is a key step because of component dynamics. Indeed, it is difficult to control accurately the position of the micropart between the fingers during grasping which can cause contact with one finger before the other and consequently the loss of the micropart. Furthermore, a risk of breaking microparts is possible if the gripping forces are not controlled.
- *insertion*: in this task, the micropart is inserted into the grooves of microassembly substrate. This task will be performed using Stereovision CAD model based visual tracking.
- *guiding*: is essential to perform precise positioning. However, the uncertainties on the alignment between the axes of guiding and the rail axis may cause undesired contacts and consequently the micropart may be loosen or broken.
- *releasing*: is critical due to pull-off forces inducing sticking effects and probably causing the loss of the micropart.

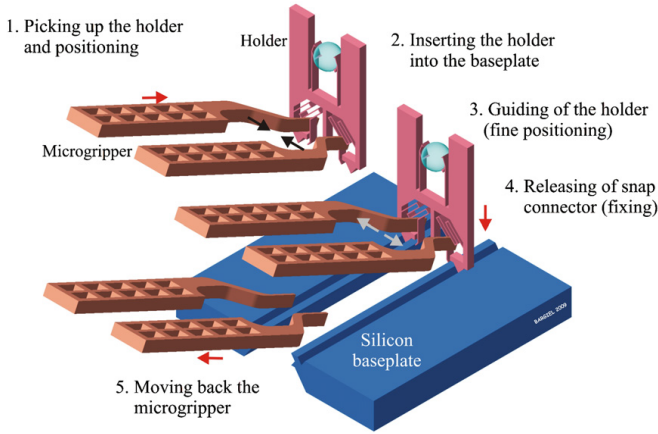


Fig. 4: The steps of microassembly for complex MOEMS presented in [13].

III. AUTOMATED MANIPULATION AND INSERTION USING CAD MODEL BASED VISUAL TRACKING

The objective of this task is to manipulate the microcomponent towards a desired position and to insert the microcomponent inside the V-grooves of the rails. Indeed, microassembly robotic station has several cameras allowing to visualize and locate the microcomponents relative to the substrate. The first step is to recognize the manipulated microcomponent. In this paper, we have chosen to locate the microcomponent using its CAD model. Then, the position of the microcomponent should be determined in the robot frame. The stereoscopic vision technique is used which consists of using two cameras to reconstruct the position of the microcomponent. Consequently, the control of the robot can be done to position the microcomponent in its desired position.

A. Component tracking

The component tracking is possible due to the interface between two cameras with the computer and the use of a library called *cvlink* enabling to use OpenCV on Matlab. This library allows to realize successive steps as display a picture, crop it, apply filters to extract the component contour. Then, the ViSP library is used to extract the 3D coordinates of the manipulated component and to track the angles which allow to deduce the characteristics of the CAD model of the component (Fig. 5). Reference [4] describes the implementation method for doing this.

B. Determination of the position of the microcomponent

Each camera allows to have the position of the component in its frame. In order to calibrate visual system, the transformation matrix (${}^{c_2}M_{c_1}$) between cameras frames has to be estimated. This matrix allows to represent the object position obtained with the first camera (R_{c_1}) in (R_{c_2}). This matrix can be found using world frame (R_w) as an intermediary stage, that gives the following equation:

$${}^{c_2}M_{c_1} = {}^{c_2}M_w {}^wM_{c_1} = {}^{c_2}M_w ({}^{c_1}M_w)^{-1} \quad (1)$$

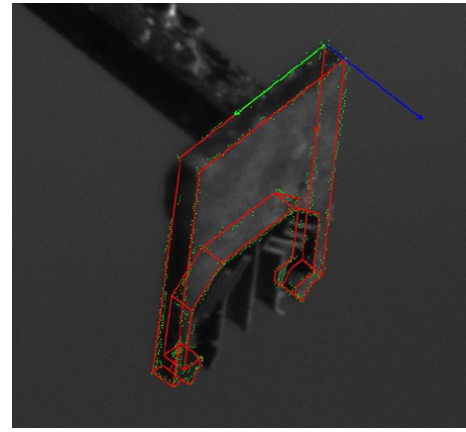


Fig. 5: Image showing the contour detection of the microcomponent.

Index w represents world frame or robot frame. Matrices ${}^{c_2}M_w$ and ${}^{c_1}M_w$ represent the transformation matrices between respectively cameras C_1 and C_2 frames and the world frame. Fig. 1 illustrates the different transformation matrices. A calibration is done to determine the coefficient of these

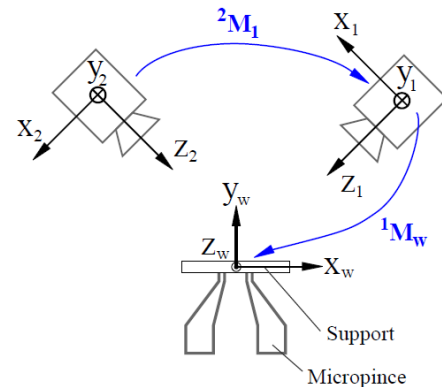


Fig. 6: Representation of changing frames matrix.

two matrices. Indeed, the component is grasped with the microgripper, then, it is moved in the field of view of the two cameras. Meanwhile, three complementary information is recorded: the video stream from each camera and the position measurement of the robot (each robot axis has an internal position sensor). An optimization algorithm is then used to minimize the distance between the pose obtained by the tracker and those obtained by the sensors of the robot axis in camera frame along 3D planned path.

C. Visual Servoing

Once the system calibration is done, it is possible to correctly measure the 3D position of the object. So, the control law can be developed to move the robot and position the component in its desired position in the rail. Among existing types of visual servoing, PBVS (Position Based Visual Servoing) was chosen for the following reasons: first, because using visual tracking techniques we obtain directly

the 3D object position. Its main advantage consists in the fact that the set point for control loop can be expressed in Cartesian coordinate system. Secondly, using PBVS one obtain better robot behavior in Cartesian space contrary to Image Based Visual Servoing (in image plane). So, as an input of control loop, we use a 3D pose, which represents the desired position of the object, s^* . Current object position in every iteration will be noted as $s(t)$. The both quantities are expressed in R_{c_1} . A visual servoing control law consists in minimizing the error between the current pose $s(t)$ and the desired pose s^* as shown in Fig. 7. Experimental investigations have shown that this technique

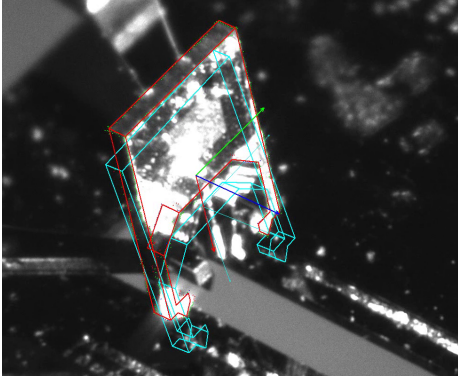


Fig. 7: Image acquired with the camera c_1 with current pose (red) and desired pose (blue).

can position the microcomponent to its desired position with a positioning error less than $5 \mu\text{m}$ along three axis space in several seconds (speed accuracy trade-off). More details of this control technique and its stability have been presented in [17], [18].

IV. AUTOMATED MICROASSEMBLY USING HYBRID FORCE/POSITION CONTROL

This approach enables to perform the microassembly by combining both position and force information. The force information is critical at the microscale due to the predominance of surface and contact forces. Indeed, during microassembly, any contact between two surfaces (microgripper and microcomponent or microcomponent and microassembly substrate) induces sticking effect called pull-off force. This specificity induces more complexity in the microassembly process. In this section, automated microassembly is performed using the experimental setup shown in section II where the force measurement is performed using the two end-effectors of the TSMF. Then, an hybrid force/position control law is developed to automated grasping, guiding and releasing tasks.

The hybrid force/position control has been introduced by Raibert and Craig in [19]. It is among the most relevant control techniques for the assembly (at the macroscale) where spaces with constrained motion and free motion exist and where the force and position need to be controlled along different axis. The hybrid force/position formulation requires

to combine two controls: some axis are controlled in position and others are controlled in force. The separation is done using a selection matrix \mathbf{S} which determines the position controlled axis and the matrix $\mathbf{I-S}$ which determines the force controlled axis.

Inspired from the classical hybrid force/position control, a control scheme is proposed as in Fig. 8. According to Fig.

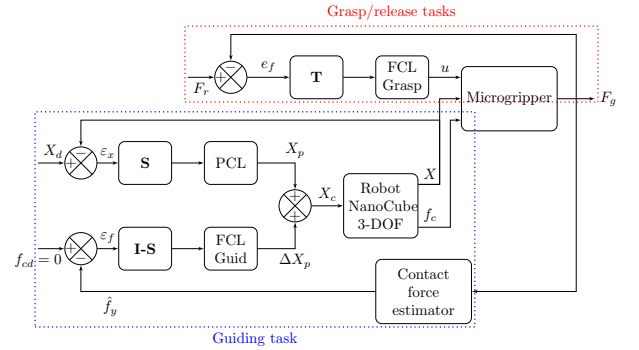


Fig. 8: Hybrid force/position control diagram used for the automation of three microassembly tasks (grasping, guiding and releasing).

8, the control scheme is divided into two parts. The first part is used to automate the grasping and releasing tasks where the microgripper is controlled. The bloc \mathbf{T} is a switch for the task specification. It enables to switch between the grasp and the release of the components tasks and the guiding task. It has two possible values 0 for the guiding task and 1 for grasp and release tasks. FCL corresponds to the force control law and will be presented in the following. $F_r = (F_{r_1}, F_{r_2})$ and $F_g = (F_{g_1}, F_{g_2})$ are two vectors to represent the two reference forces and the two gripping forces. e_f is the force error between the reference gripping force and the applied gripping force.

When the micropart is grasped at the desired force, the controller switches to second part where the switch \mathbf{T} is set to zero enabling to automate the guiding task where the positioning stage is controlled and the microgripper is not controlled. PCL corresponds to the position control law which is the internal controller of the positioning stage. FCL is the force control law. $X_d = (x_d, y_d, z_d)$ is a vector for the desired positions along the three axis X, Y and Z. f_{c_d} is the desired contact force which is generally null because no contact between the micropart and the substrate is envisaged while the guiding task. f_y and \hat{f}_y are respectively the contact force and its estimation using the method developed in [10]. ϵ_x and ϵ_f are respectively the position error and the force error between the desired contact force and the estimated force. X_p is the output of the PCL. The output of the FCL, ΔX_p , is added to X_p in order to determine X_c which is the position command of the robot positioning stage. $X_c = X_p + \Delta X_p$. X is the measured position of the positioning stage using the internal sensors of the NanoCube. PCL is the internal control loop of the positioning stag.

FCL is a sliding mode impedance control and it is used

to control not only the force interaction but also the dynamic interaction between different components (microgripper, microcomponent and microassembly substrate). Using this control technique, a desired dynamics relation between the applied force and the displacement is set for the control law and the objective of the controller is to follow the desired dynamic relation and to track the force to the desired force. The importance of controlling the dynamics is that it enables to perform high speed microassembly process. The details of the sliding mode impedance control technique are presented in [20] where high speed guiding tasks have been performed. Guiding speeds of 5 mm/s have been reached while reducing undesired contact dynamics.

V. EXPERIMENTAL RESULTS

In this section, experimental results for both control approaches presented in sections III and IV are performed to validate the approach. The final goal is to perform complete automated microassembly process. First, the micropart is grasped using the control law shown in section IV, then it is inserted in the V-grooves of the microassembly substrate using stereovision based CAD-model based visual tracking as shown in section III. The results of the automated insertion are presented in Table II and Fig. 9. After doing several

TABLE II: Mean absolute errors of assembly before and after releasing the object.

Mean assembly error	Before releasing	After releasing
e_x	3.07 μm	9.88 μm
e_y	3.56 μm	8.91 μm
e_z	4.63 μm	6 μm

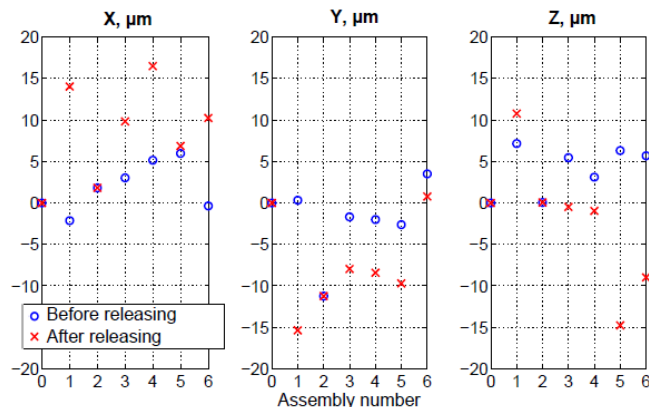


Fig. 9: Assembly errors due to the step of component release measured by visual system in R_w .

consecutive automated assemblies, one can notice that the mean absolute positioning error (Fig. 9, Table II) before holder releasing is inferior to 5 μm . The error becomes bigger compared to visual servoing error, because during assembly the object comes into contact with a silicon base plate that results in uncontrollable rotations of the object that cannot be compensated using our robot structure. The

mechanical structure of the holder was developed in a sort that while releasing it can compensate angular position errors thanks to the particular form of the object and the base plate: when snap connector is released one can observe "fastening" between objects. However, after several experiments, we can notice that angular errors are compensated only partially. This effect of "fastening" also results in change of object position that explains the increasing errors.

The visual servoing technique enables to perform pre-positioning of the microcomponent with errors less than 10 μm . To reduce the effect of positioning error using visual servoing, a cycle of automated grasping, guiding inside the rail and releasing is performed using hybrid force/position control (section IV) to perform fine positioning of the micropart. The results of this approach is shown in Fig. 10. First, the position of the micropart is determined from

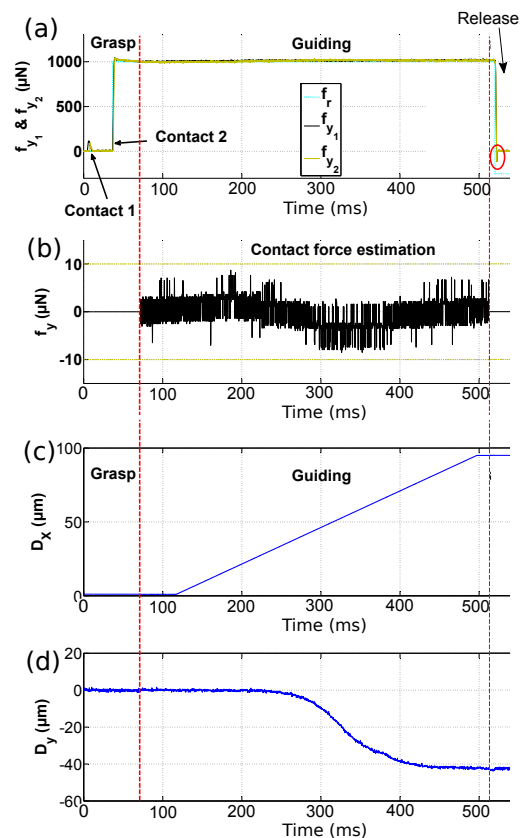


Fig. 10: Experimental results for an automated microassembly sequence of a micropart showing: (a) the gripping force (F_{y_1} and F_{y_2}), (b) lateral contact force (f_y) estimation, (c) Nanocube displacement along the X axis (D_x) and (d) NanoCube displacement along the axis of correction Y (D_y).

each side of the microgripper (contact 1 of Fig. 10), then, a desired force is applied to the controller and grasp is performed in 20 ms. Then, the guiding task starts to position the component in its desired position with precision less than 1 μm with high speed up to 5 mm/s while keeping the contact force to zero (\hat{F}_y in Fig. 10) thanks to high dynamic control

using sliding mode control. When the component is in its position, a negative force reference is applied to separate the contact between the component and the microgripper fingers in presence of pull-off force.

The result of microassembly of several optical microcomponent is shown in Fig. 11.

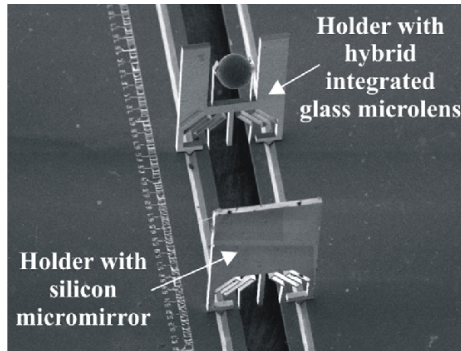


Fig. 11: Example of the assembly of flexible optical components to realize hybrid MOEMS.

VI. CONCLUSIONS

This paper studies the fabrication of hybrid microcomponents through automated robotic microassembly which is a relevant approach for fabrication of complex structures at the microscale. The approach used in this paper is to combine the use of robotic structure and an active microgripper with sensorized end-effectors to realize complex microassembly tasks. The robotic station used for the microassembly has been presented in this paper and its use for the assembly of flexible optical microcomponents has been done as a case study. The automated microassembly has been done for better repeatability and accuracy of the tasks and to reduce the time cycle. For this reason, two complementary techniques have been proposed and presented in this paper. The first technique is to realize automated insertion using stereovision CAD-model based visual tracking. This technique enables to position the microcomponent in the microassembly process with errors less than $10\ \mu\text{m}$. Then, to reduce the positioning errors using the first technique, hybrid force/position control is proposed to perform automated grasping, guiding for repositioning of the component and releasing tasks. The hybrid force/position control proposed in this paper enable to perform grasping, guiding and releasing tasks in less than 1 s despite microscale specificities. As a result of this paper, complete automated microassembly process is performed leading to precise positioning of complex flexible optical component with accuracy less than $1\ \mu\text{m}$.

ACKNOWLEDGMENT

These works have been funded by the Franche-Comté region, supported by the Labex ACTION project (contract "ANR-11-LABX-0001-01") and by the French RENATECH network through its FEMTO-ST technological facility. The authors would like also to thank Sylwester Bargiel and

Christophe Gorecki for their collaboration in the fabrication of optical bench.

REFERENCES

- [1] D. Tolfree and M. Jackson, *Commercializing Micro-Nanotechnology Products*. CRC Press, 2006.
- [2] E. Avci, K. Ohara, C.-N. Nguyen, C. Theeravithayangkura, M. Kojima, T. Tanikawa, Y. Mae, and T. Arai, "High-speed automated manipulation of microobjects using a two-fingered microhand," *IEEE Trans. on Industrial Electronics*, vol. 62, no. 2, pp. 1070–1079, Feb. 2015.
- [3] J. Wason, J. Wen, J. Gorman, and N. Dagalakis, "Automated multiprobe microassembly using vision feedback," *IEEE Trans. on Robotics*, vol. 28, no. 5, pp. 1090–1103, Oct. 2012.
- [4] B. Tamadazte, E. Marchand, S. Dembélé, and N. L. Fort-Piat, "Cad model-based tracking and 3d visual-based control for mems microassembly," *The International Journal of Robotics Research*, 2010.
- [5] Y. Anis, M. Holl, and D. Meldrum, "Automated selection and placement of single cells using vision-based feedback control," *IEEE Trans. on Automation Science and Engineering*, vol. 7, pp. 598 – 606, July 2010.
- [6] L. Wang, L. Ren, J. Mills, and W. Cleghorn, "Automated 3-d micrograsping tasks performed by vision-based control," *IEEE Trans. on Automation Science and Engineering*, vol. 7, pp. 417 – 426, 2010.
- [7] Z. Lu, P. C. Y. Chen, A. Ganapathy, G. Zhao, J. Nam, G. Yang, E. Burdet, C. Teo, Q. Meng, and W. Lin, "A force-feedback control system for micro-assembly," *J. of Micromech. Microeng.*, vol. 16, no. 9, p. 1861, September 2006.
- [8] M. Rakotondrabe and I. Ivan, "Development and force/position control of a new hybrid thermo-piezoelectric microgripper dedicated to micromanipulation tasks," *IEEE Trans. on Automation Science and Engineering*, vol. 8, no. 4, pp. 824–834, Oct. 2011.
- [9] Y. Xie, D. Sun, H. Y. G. Tse, C. Liu, and S. H. Cheng, "Force sensing and manipulation strategy in robot-assisted microinjection on zebrafish embryos," *IEEE/ASME Trans. on Mechatronics*, vol. 16, no. 6, pp. 1002–1010, Dec. 2011.
- [10] B. Komati, K. Rabenorosoa, C. Clévy, and P. Lutz, "Automated guiding task of a flexible micropart using a two-sensing-finger microgripper," *IEEE Trans. on Automation, Science and Engineering*, vol. 10, no. 3, pp. 515–524, July 2013.
- [11] W. Zhang, A. Sobolevski, B. Li, Y. Rao, and X. Liu, "An automated force-controlled robotic micromanipulation system for mechanotransduction studies of drosophila larvae," *IEEE Trans. on Automation Science and Engineering*, vol. PP, no. 99, pp. 1–9, 2015.
- [12] K. Rabenorosoa, C. Clévy, P. Lutz, M. Gauthier, and P. Rougeot, "Measurement of pull-off force for planar contact at the microscale," *Micro Nano Letters*, vol. 4, pp. 148 –154, 2009.
- [13] S. Bargiel, K. Rabenorosoa, C. Clévy, C. Gorecki, and P. Lutz, "Towards micro-assembly of hybrid moems components on a reconfigurable silicon free-space micro-optical bench," *J. of Micromech. Microeng.*, vol. 20, no. 4, p. 045012, April 2010.
- [14] B. Komati, C. Clévy, and P. Lutz, "High bandwidth microgripper with integrated force sensors and position estimation for the grasp of multi-stiffness microcomponents," *IEEE/ASME Trans. on Mechatronics*, vol. PP, no. 99, DOI: 10.1109/TMECH.2016.2546688 2016.
- [15] P. de Lit, J. Agnus, C. Clévy, and N. Chaillet, "A four-degree-of-freedom micropreheensible microrobot on chip," *Assembly and Automation*, vol. 24, no. 1, pp. 33–42, 2004.
- [16] B. Komati, J. Agnus, C. Clévy, and P. Lutz, "Prototyping of a highly performant and integrated piezoresistive force sensor for microscale applications," *J. of Micromech. Microeng.*, vol. 24, no. 3, p. 035018, March 2014.
- [17] A. Kudryavtsev, G. Laurent, C. Clévy, B. Tamadazte, and P. Lutz, "Analysis of cad model-based visual tracking for microassembly using a new block set for matlab/simulink," *Int. J. of Optomechatronics*, vol. 9, no. 4, July 2015.
- [18] —, "Stereovision-based control for automated moems assembly," *IEEE/RSJ Int. Conf. on Intelligent Robots and Systems*, pp. 1391–1396, Sept 2015.
- [19] M. Raibert and J. Craig, "Hybrid position/force control of manipulators," *Trans. of ASME, J. of Dynamic Systems, Measurement, and Control*, vol. 102, pp. 126–133, 1981.
- [20] B. Komati, "Automated microassembly using an active microgripper with sensorized end-effectors and hybrid force/position control," Ph.D. dissertation, University of Franche-Comté, Dec. 2014.